Influence of Biofuel Blending on Inorganic Constituent Behavior and Impact in Fluidized-Bed Gasification

Florian Lebendig [a*], Michael Müller [a]

[a] Forschungszentrum Jülich, Institute of Energy Materials and Devices (IMD-1), Wilhelm-Johnen Str., 52428 Jülich, Germany

[*]Corresponding author. E-mail address: f.lebendig@fz-juelich.de

Abstract

A promising technology for producing carbon-neutral fuels is fluidized-bed gasification of biomass. When combined with chemical looping technology (CLG), the process becomes even more efficient. However, using biomass-based fuels can lead to significant ash-related issues, including bed agglomeration, fouling, deposition, slagging, and high-temperature corrosion. To address these issues, several biomass upgrading approaches are used to improve the quality of the feedstock for gasification. These approaches include torrefaction, water-leaching, and blending with different additives. This study focuses on the influence of additives and biomass co-blending with low-cost biofuels on the behavior of inorganic constituents and under gasification-like conditions at 950 °C and the corresponding impact in fluidized-bed gasification. For example, blending (upgraded) barley straw with 2 wt% $CaCO_3$ resulted in a decrease in slag and a corresponding increase in the proportion of solid oxides. This indicates that thermal stability can be expected at operating temperatures up to 950 °C. Similarly, adding Ca/Si-rich biowaste components increases the ash softening point of herbaceous biofuels. Furthermore, the results show that adding Ca-based or woody biofuel components has a chemical effect on the fate of volatile inorganics. For example, increasing the concentration of calcium in the fuel significantly reduces the release of HCl and partially reduces the release of sulfur species, thus reducing the corrosion risk. These results contribute to the development of more efficient and cleaner biomass gasification processes for producing carbon-neutral fuels.

Keywords

Ash fusion, Biofuels, Pre-treatment, Gasification, High-temperature corrosion, Slagging

Nomenclature

Abbreviations

+ A or w/o A	With added additive ($CaCO_3$) or without additive
Ca	Calcium
CLG	Chemical Looping Gasification
HSM	Hot Stage Microscopy
ICP-OES	Inductively Coupled Plasma Optical Emission Spectroscopy
kN	Kilonewton

MBMS	Molecular Beam Mass Spectrometer
OB	Oak bark
PB	Pine bark
PFR	Pine forest residues
To	Torrefied
T&P / To-WL	Torrefied and postwashed
WL	Water-leached
WL-To	Prewashed and torrefied
Symbols and units	
m/z	Mass-to-charge ratio
vol%	Volume percentage
wt%	Weight percentage

1. Introduction

The global energy demand is consistently increasing due to population growth, and it continues to rely predominantly on fossil fuels. The Paris Agreement emphasizes the need to limit global warming to below 2 °C, preferably 1.5 °C [1]. As a response, there is a gradual shift towards renewable energy, aiming to replace fossil fuels, accounting for approximately 45% of total CO_2 emissions as of 2020 [2]. In comparison to other renewable sources like wind, solar, or hydroelectric power, biomass holds great promise due to its topographical independence and abundant availability [3].

Among other fluidized bed gasification technologies, chemical looping gasification (CLG) is recognized as a promising technology for converting biomass into synthetic fuels [4]. A detailed description of the multistep process can be found elsewhere [5]. CLG is achieved through the use of two interconnected fluidized-bed reactors to improve heat and mass transfer efficiency [6–8]. Various types of fuels can be gasified in the fuel reactor by utilizing a metal oxide (Me_xO_y) as the oxygen carrier. The metal oxide is reduced (Me_xO_{y-1}) during gasification in the fuel reactor and then moved to the air reactor, where it is oxidized back to its original state using air.

During the gasification process, various challenges arise from biomass ash, including interactions between oxygen carriers and inorganic trace elements, when the system is combined with chemical looping technology, as well as agglomeration and fouling in the fuel reactor, which is relevant for all types of fluidized-bed systems. These issues can lead to operational difficulties and damage to plant components. Therefore, a thorough understanding of ash chemistry is essential to minimize the risks associated with ash. Biofuel upgrading can be employed to mitigate these risks. Although ash-related issues in biomass gasification systems are generally assumed to be similar to those in combustion processes [9], the explicit behavior of new biomass fuels under gasification conditions is not well-defined. Hence, a comprehensive fuel characterization focusing on gasification-related properties becomes crucial for their integration.

Torrefaction is a viable method for reducing transportation costs and producing feedstocks with desirable physical properties, such as increased bulk density. Additionally, torrefaction has been found to significantly

decrease the amount of chlorine in feedstocks [10], resulting in lower levels of alkali chlorides. Water-leaching treatment is an effective method for removing alkali metal salts, including chlorides, carbonates, and sulfates due to their high solubility. In a previous study conducted by Meesters et al. [11], extraction experiments demonstrated that four consecutive water extraction steps reduced chloride and potassium concentrations by approximately 80% and 90%, respectively, bringing them within acceptable limits or close to them.

Carefully selecting additives for biomass or fuel blending with low-cost biowaste materials, such as woody feedstocks, offers a promising approach to modify the chemical composition and physical properties of the biofuel, thereby significantly mitigating ash-related risks. This can enable control of the ash melting behavior and release behavior of inorganic species under gasification conditions. The coal industry has successfully employed blending techniques to meet emission targets and minimize ash production during power generation [12–14], thereby affecting feedstock quality. Feedstock blending is a widely recognized and effective approach to address ash-related challenges, which vary significantly due to compositional variations [15, 16]. In terms of ash melting behavior, calcium (Ca) and magnesium (Mg) are known to increase the ash melting temperature, while sodium (Na) and potassium (K) decrease it [17, 18]. Additionally, low-melting alkali- and alumina silicates and chlorides can significantly decrease the ash melting point [16]. Previous studies have demonstrated that the addition of oxides or inorganic salts to the initial biomass can enhance its melting behavior and alter its thermal characteristics [19–21].

Based on the understanding of the $CaO\text{-}K_2O\text{-}SiO_2$ system, knowledge about fusibility tendencies can be utilized to predict and optimize feedstock quality [22]. Through blending, the ratio of problematic constituents can be adjusted, thereby improving the overall quality of the feedstock.

Ray et al. [23] have highlighted the potential of blending and densification processes to enable more cost-effective downstream processing. By utilizing multiple biomass types through blending, the overall land base available for biomass production can be increased, leading to lower total costs for biorefinery feedstock and shorter transportation distances [24]. Recent studies have also emphasized the opportunity to deliver satisfactory feedstock for biorefineries at lower costs by blending high-quality feedstocks with marginal-quality feedstocks [25–27].

However, lignocellulosic biomass feedstocks are diverse, making it challenging to define a general pre-treatment process applicable to all of them [28]. While many research studies have focused on analyzing fuel properties through washing, thermal treatment, or torrefaction [29–31], there are limited studies available on the combination of these methods with additive blends [32]. It is crucial to thoroughly investigate and develop the use of blended, densified, and water-leached feedstocks in thermochemical conversion processes, instead of conventionally ground biomass from a single source.

In this study, various investigation techniques have been employed to understand the influence of blending and additivation on the bahavior of inorganics. Molecular Beam Mass Spectrometry (MBMS) was utilized to investigate the release and fate of inorganic volatile species under gasification-like conditions at 950 °C. Hot stage microscopy (HSM) was used to examine the ash fusion characteristics. Lab-scale experiments were complemented with thermodynamic modeling using FactSage™ to predict the release behaviour and mineral phase formations in

the ash. Based on the findings, specific conclusions regarding the risks of bed agglomeration, slagging, fouling, and high-temperature corrosion in a fluidized-gasifier operated at 950 °C were drawn.

2. Materials and methods

2.1. Materials and biofuel upgrading

The herbaceous feedstocks wheat, barley, corn, and colza straw were purchased commercially from Futtermittel Louven, Germany. The effect of different pre-treatment methods, such as torrefaction and water-leaching, on the behaviour of inorganics of these feedstocks was already investigated in a previous study [33]. In the present work, they were further improved by blending them with either calcium carbonate or woody biofuel components. Using FactSage^{TM}, preliminary model calculations were conducted to create various sample blends with oak bark (OB), pine bark (PB), or pine forest residues (PFR). In addition to these woody blend components, ground limestone ($CaCO_3$) was selected as a calcium-based additive. It is important to note that the weight ratio between the additive and the pre-treated fuel itself, not the ash, is considered for both the woody components and the Ca-additive.

In the present study, straw pre-treated like in our previous study [33] was used. The samples underwent a two-step washing process, where each cycle lasted one hour. The sample-water mixture, comprising 50 g biomass and 0.5 l deionized water, was continuously mixed throughout the washing process. Furthermore, samples were torrefied in a pure argon 5.2 atmosphere at a temperature of 250 °C for a duration of 1 hour.

Three sample series were created to study the effects of different fuel blending approaches. Firstly, the impact of adding limestone (commercial quality) as an additive to pre-treated barley straw was investigated. Secondly, the effect of different proportions of PB (10 wt% to 90 wt%) as a co-blending component with colza straw was investigated. The final sample series focused on blending various pre-treated fuels with woody components. These blends were chosen based on promising results from preliminary equilibrium calculations. These calculations involved predicting ternary phase diagrams ($CaO–K_2O–SiO_2$) to estimate the solid ash composition of each sample blend at a temperature of 950 °C. The temperature was set at 950 °C to ensure comparability with previous research studies [32–34], which were related to CLG utilizing the same un-blended biofuels.

2.2. Chemical characterization

The samples were analyzed on their elemental composition with a CHNS analyzer and optical emission spectroscopy combined with inductively coupled plasma (ICP-OES) for the major ash forming elements. Microwave acid digestion of the fuels was applied prior to the determination by ICP-OES [32], [33]. Each fuel sample was milled and sieved to a diameter of 0.86 mm to enhance analytical investigations in subsequent steps.

2.3. Experimental hot gas analysis by molecular beam mass spectrometry (MBMS)

The inorganic gaseous species released during gasification were determined in real-time using Molecular Beam Mass Spectrometry (MBMS). A detailed description of the experimental setup can be found in previous publications [35, 36].

Gasification experiments were conducted under gasification-like conditions at a temperature of 950 °C. A four-zone furnace was utilized, with a corundum tube inside the furnace directly connected to the MBMS inlet nozzle. The gasification of the sample occurred in the first two zones at 950 °C. A temperature zone of 1400 °C was set to crack any formed hydrocarbons, ensuring that only inorganic species were investigated.

A total of three measurements were performed for each sample, and the results were averaged for semi-quantitative analysis and error calculations. Similar atmospheric conditions as the ashing procedure were maintained throughout the measurement campaign, which included 15 vol% H_2O-steam and 5 vol% CO_2 in helium. The total gas flow was set to 4 L/min for each experiment. A 50 mg fuel sample was gasified in a single run. The samples remained in the furnace for varying retention times, typically ranging from 2 minutes to a maximum of 6 minutes, based on an initial overview of all spectra. The retention time reflected the reaction sequence, as different species exhibit distinct release behaviors, specifically devolatilization, and subsequent char gasification and ash reactions. Intensity-time profiles of $^{23}CO_2^{++}$, $^{34}H_2S^+$, $^{35}Cl^+$, $^{36}HCl^+$, $^{37}Cl^+$, $^{38}HCl^+$, $^{39}K^+$, $^{47}PO^+$, $^{55}KO^+$, $^{58}NaCl^+$, $^{60}COS^+$, $^{62}P_2^+$, $^{63}PO_2^+$, $^{64}SO_2^+$, $^{74}KCl^+$, $^{81}Na_2Cl^+$, $^{97}NaKCl^+$, $^{113}K_2Cl^+$, $^{126}P_2O_4^+$, and $^{142}P_2O_5^+$ were recorded and normalised to the $^{23}CO_2^{++}$ base level signal for quantification.

2.4. Ash fusion testing

The ash of each sample was generated under gasification-like conditions at a constant temperature of 550 °C. The gasifying medium consisted of 15 vol% H_2O-steam in N_2, and 5 vol% CO_2. At the start of the process, a small amount of oxygen was introduced to facilitate carbon conversion. A lambda sensor was used to control the partial pressure of oxygen throughout the ashing procedure. When it increased, the oxygen supply was stopped to prevent combustion. Afterwards, the ash samples were annealed at 550 °C for 3 hours in argon-hydrogen (4% H_2 in Ar) to ensure the formation of crystalline compounds. For the determination of ash melting behavior using hot stage microscopy (HSM), the ash was pressed into a cylindrical pellet with a diameter of 5 mm, achieving a strength of approximately 1.5 kN. A drop of pure isopropanol was added as a surfactant to maintain stability of the pellet during the pressing process. The height of the sample pellet varied between 4 mm and 7 mm. The same amount of ash was weighed for each sample preparation. The evaluation was based on the ratio of current sample height/original sample height (coefficient h_x/h_0) according to Pang et al. [37].

2.5. Thermodynamic equilibrium calculations

Thermodynamic equilibrium calculations using the computational package FactSage™ 7.3 [38] were conducted to predict the formation of inorganic mineral phases of ash constituents under gasification conditions. The commercial database SGPS and the GTOX database [39] were used for this study. Thermodynamic equilibrium calculations were conducted considering the chemical compositions of the corresponding fuel ashes presented in Table 1. The phase formations in the ash under gasification conditions were calculated considering

the addition of water (steam/feedstock = 0.5 g/g) and oxygen (Fe_2O_3/feedstock = 0.48 g/g, only the oxygen of the oxygen carrier Fe_2O_3 was taken into account to exclude possible reactions between oxygen carrier and ash, which were not in the focus of the present investigation).

3. Results and discussion

3.1 Fuel composition

Table 1 presents the ultimate analyses of the fuel sample blends.

Table 1

Ultimate analysis of the fuel blend sample series in wt% or mg kg^{-1}. Note that the composition of the biofuel blends is determined based on the characterization of the raw or upgraded fuels themselves, as presented in their raw form in [32, 33]. All compositions were calculated on a percentage basis. For upgraded barley straw blended with 2 wt% $CaCO_3$, only the value for Ca was determined on a molar basis, as 2 wt% $CaCO_3$ (100.09 g/mol) corresponds to 0.8 wt% Ca (40.08 g/mol).

Upgraded barley straw blended with 2 wt% $CaCO_3$.

wt%	**Untreated (reference)**	**Torrefied**	**Water-leached**	**Torrefied, postwashed**	**Prewashed, torrefied**
C	43.5	50.5	44.5	47.3	49.7
H	6.20	5.91	6.37	5.85	5.95
N	0.56	0.73	0.39	0.37	0.63
O	44.8	38.7	45.7	40.7	41.2
S	0.13	0.12	0.10	0.10	0.10
mg kg^{-1}	Ash forming components (major elements only)				
Cl	618	1076	42	60	100
Al	20	20	20	40	20
Ca (fuel)	3010	4310	2820	4400	4130
Ca (additive)	8009	8009	8009	8009	8009
Fe	7	7	7	49	7
K	15600	19550	3600	7170	4610
Mg	377	550	271	515	405
Na	90	140	90	200	90
P	890	1258	490	980	1010
Si	7480	10720	7000	10710	10800

Feedstocks for fuel blending (T&P = torrefied and postwashed, OB = oak bark, PB = pine bark, PFR = pine forest residues).

wt%	**Untreated Colza**	**T&P Barley**	**T&P Corn**	**T&P Colza**	**T&P Wheat**	**PFR**	**PB**	**OB**

C	41.2	47.1	48.1	47.6	49.3	52.7	42.1	45.5
H	6.01	5.85	5.90	5.98	5.83	6.40	5.66	6.22
N	0.51	0.37	0.57	0.36	0.47	0.34	0.40	0.43
O	44.1	39.7	40.3	42.2	39.4	40.5	38.7	43.4
S	0.33	0.10	0.10	0.10	0.10	0.05	0.10	0.10
mg kg^{-1}	Ash forming components (major elements only)							
Cl	8340	60	273	349	298	70	232	63
Al	31	40	550	40	61	174	830	239
Ca	8430	4400	3110	4760	2640	3390	7600	15560
Fe	7	49	270	18	76	134	830	158
K	22370	7170	4470	3250	6400	1370	1840	2810
Mg	552	515	1740	253	588	453	676	516
Na	1199	200	100	200	200	34	228	2810
P	242	980	573	130	210	217	409	368
Si	98	10710	10800	70	10200	958	9200	3880

Torrefied and postwashed straw blended with woody biofuel component (wt% / wt%).

wt%	**Barley/OB 65/35**	**Corn/PB 70/30**	**Corn/PFR 60/40**	**Colza/PB 65/35**	**Wheat/PFR 60/40**	**Wheat/OB 60/40**
C	46.5	46.3	49.9	45.7	50.7	47.8
H	5.98	5.83	6.10	5.87	6.06	5.99
N	0.63	0.52	0.48	0.37	0.42	0.45
O	41.0	39.8	40.4	41.0	39.8	41.0
S	0.10	0.10	0.08	0.10	0.08	0.10
mg kg^{-1}	Ash forming components (major elements only)					
Cl	61	261	192	308	207	204
Al	110	634	400	317	106	132
Ca	8306	4457	3222	5754	2940	7808
Fe	87	438	216	302	99	109
K	5644	3681	3230	2757	4388	4964
Mg	515	1421	1225	401	534	559
Na	1114	138	74	210	134	1244
P	766	524	431	228	213	273
Si	8320	10320	6863	3266	6503	7672

Untreated colza straw blended with pine bark (wt% / wt%).

wt%	**Colza/PB 90/10**	**Colza/PB 75/25**	**Colza/PB 50/50**	**Colza/PB 25/75**	**Colza/PB 10/90**
C	41.3	41.4	41.7	41.9	42.0

H	5.98	5.92	5.84	5.75	5.70
N	0.50	0.48	0.46	0.43	0.41
O	43.6	42.8	41.4	40.1	39.2
S	0.31	0.27	0.22	0.16	0.12
mg kg^{-1}	Ash forming components (major elements only)				
Cl	7529	6313	4286	2259	1043
Al	111	231	431	630	750
Ca	8347	8223	8015	7808	7683
Fe	89	213	419	624	748
K	20317	17238	12105	6973	3893
Mg	564	583	614	645	664
Na	1102	956	714	471	325
P	259	284	326	367	392
Si	1008	2374	4649	6925	8290

3.2 Release of inorganic constituents

The release of inorganic compounds was investigated during the pyrolysis/devolatilization phase and ash char reaction phase at 950 °C. Fig. 1 shows the semi-quantitative gas phase analysis results for the blended samples under gasification-like conditions. A comparison between upgraded barley straw with 2 wt% $CaCO_3$ (Fig. 1a) and without the additive, as studied in [33], showed differences in the release of inorganic species.

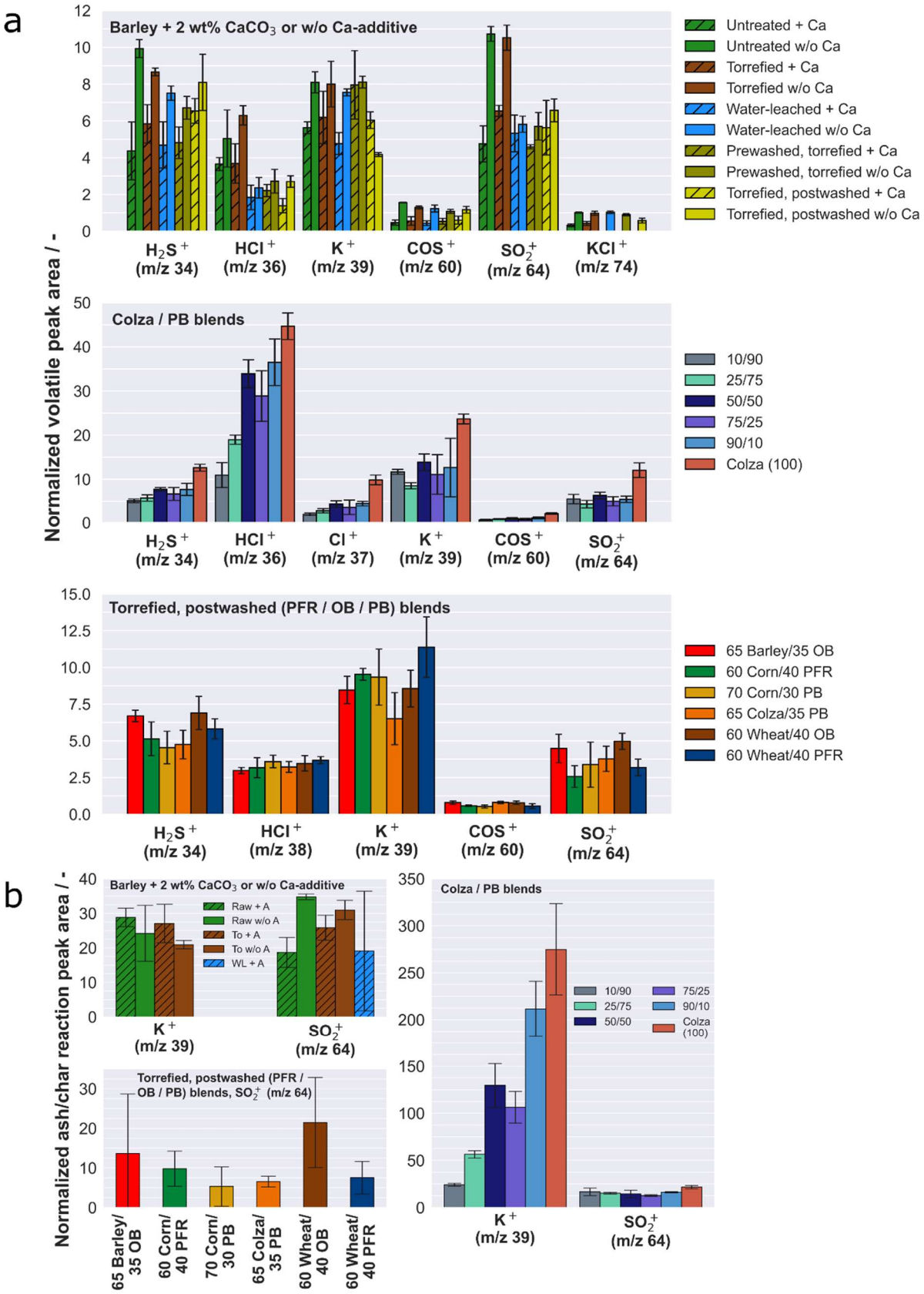

Fig. 1. Release of inorganics during gasification-like conditions. **a** Averaged normalized peak areas of detected inorganics during pyrolysis/devolatilization phase at 950 °C. Top: upgraded barley straw blended with and w/o 2 wt% $CaCO_3$, center: untreated colza straw co-blended with PB, bottom: torrefied and postwashed straw varieties, co-blended with varied quantities of woody blends (PFR, OB, or PB). **b** Averaged normalized peak areas of detected species released during the ash/char reaction

phase at 950 °C. Note that the non-blended components of biofuel (barley and colza straw), which have been included for comparison, were investigated in reference [33].

The Ca-blended samples exhibited lower release of sulfur species (H_2S, SO_2, and COS) during devolatilization, with a quantifiable decrease of about 50%. It needs to be noted, that due to the short residence time of released species in the reactor before sampling not all initially released SO_2 is reduced to H_2S and therefore detectable. Similar observations were found for HCl release, although the decrease was not as pronounced. Fig. 2b illustrates the correlated effect of the upgraded and Ca-blended fuels on the release of KCl and SO_2 during devolatilization.

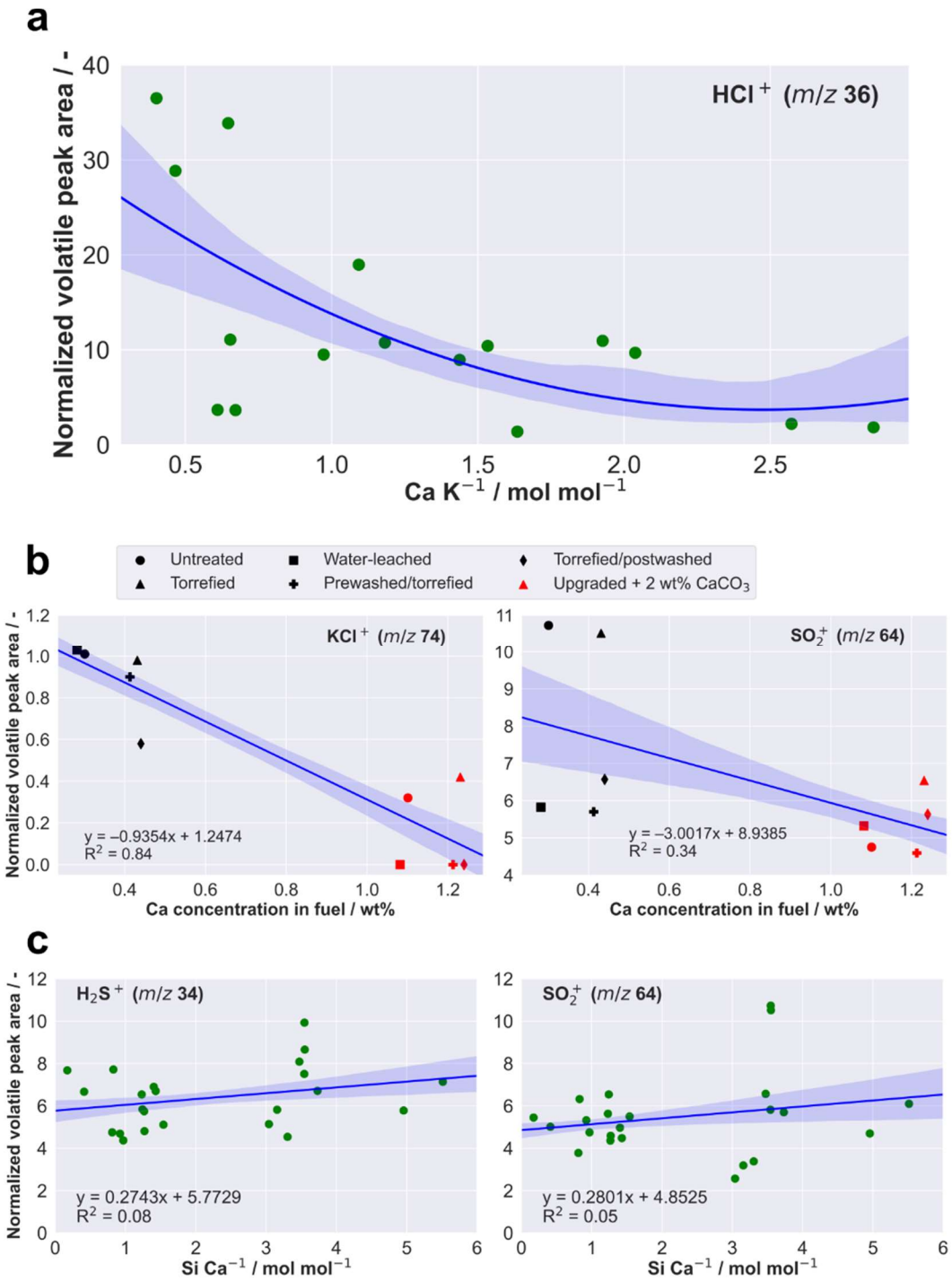

Fig. 2. Correlation between the release of inorganic species and fuel composition. **a** Summarized molar Ca/K ratio versus HCl release during devolatilization for all investigated fuel sample series in this study. **b** Correlation between the normalized peak area of KCl and SO_2 released during pyrolysis phase (upgraded barley straw blended with 2 wt% $CaCO_3$ and upgraded barley straw without additive). **c** Summarized molar Si/Ca ratio versus H_2S and SO_2 release during devolatilization for the fuel sample series and the corresponding, non-blended reference materials. Note that the non-blended components of biofuel, which have been included for comparison, were investigated in reference [33]. The confidence interval was set at 68% for **a**, **b**, and **c**.

It is clear that the samples blended with Ca-additive exhibited a significant decrease in the release of potassium chloride and sulfur dioxide. The higher the calcium content in the fuel, the lower the release of KCl or SO_2. Above a calcium content of approximately 1 wt%, hardly any KCl release was observed in the washed, pre- and postwashed samples. It is not surprising that the source material and torrefied sample without Ca-additive showed the highest release of SO_2. Water-leached, post- and prewashed samples showed the most promising results, with a 50% reduction in SO_2 release compared to raw or thermally treated material. This effect was further amplified when the upgraded samples were blended with Ca. Additionally, it was observed that Ca had a noticeable influence on the release of KCl. There is likely a cohesive interaction between K, Ca, and S species, which explains the observed mechanisms. A high potassium content in the herbaceous sample leads to retention of sulfur by the formation of potassium sulfate and suppressing SO_2 emissions. Silica binds potassium, which attenuates the formation of K_2SO_4 and promotes SO_2 release [40, 41]. The presence of calcium in the ash promotes the formation of high-melting calcium silicates, resulting in competition between K and Ca and affecting the release of SO_2. Ca acts as an S-sorbent and modifies the silica network by substituting K, thereby promoting the formation of less harmful potassium sulfate. A study by Wu et al. [42] reported on sulfates as effective additives for converting KCl to K_2SO_4 by destroying KCl. Ultimately, the formation of potassium sulfate is a promising effect, as it inherently restrains the release of both KCl and SO_2 due to the higher calcium content in the fuel. In summary, Ca exhibits two different chemical mechanisms that effectively suppress sulfur release, and similar findings have been reported for coal/straw blends under combustion conditions [40].

For the colza samples blended with different proportions of pine bark (PB), it appears that the release behavior of inorganic compounds were mainly influenced by dilution effects. Generally, it can be observed that the sample blend with 10 wt% PB exhibited similar amounts of released inorganic species compared to pure raw colza straw, as referenced in [33]. In terms of ultimate analysis, raw colza straw had a higher amount of fuel-S compared to PB. It can be noticed that the release of S-containing species such as H_2S, COS, and SO_2 increased with higher fuel-S content. Specifically, the greater the proportion of PB, the lower the quantitative amount of S-species released. The same trend was observed for both Cl species, HCl and Cl.

The last series of samples focused on investigating the influence of woody blend components on torrefied and postwashed straw samples. Based on the ultimate analyses, the following conclusions can be drawn: the torrefied and postwashed parent straw samples generally had a fuel-Ca content ranging from 0.2 wt% to 0.4 wt%, while OB and PB exhibited fuel-Ca contents of 1.6 wt% and 0.8 wt%, respectively. The fuel-K content was significantly lower for both woody components, averaging 0.2 wt% for woody materials and 0.5 wt% for the upgraded straw sample. The fuel-S content remained constant, and the fuel-Cl content was approximately the same for the upgraded fuels and the woody components. It is not surprising that fuel-Si was generally lower for the

woody materials. While OB did not affect the S and Cl species, the quantity of released S and Cl species was partially decreased compared to the upgraded straw material itself. This can likely be attributed to a dilution effect caused by OB.

In Fig. 1b, the results of the char gasification/ash reaction are presented, which typically occurs after the devolatilization phase. Specifically, for the upgraded barley straw samples with the addition of a Ca-additive, only K and SO_2 were observed to be released. The release behavior during the char gasification/ash reaction did not show any significant differences between the upgraded samples with and without the Ca-additive, as mentioned in [33]. In the samples with the additive, no further release of KCl was observed, which can be attributed to the presence of calcium, as previously discussed.

In the case of the colza/PB blends, the results for the char gasification/ash reaction align with the observations made during the devolatilization phase. A lower proportion of PB blend in colza resulted in a higher release of potassium. This can be attributed to a dilution effect, as raw PB had a lower amount of fuel-K compared to colza straw. Additionally, the Si-content in the blend is expected to have a significant effect on the release of potassium. PB has a much higher silicon content compared to colza straw, which means it can incorporate more potassium into its networks.

Regarding the release of SO_2, the ultimate analysis in Table 1 indicated a decrease in the sulfur fraction for sample blends with an increased proportion of PB. The lower fuel-S content, therefore, limited the formation of SO_x. Torrefied-postwashed wheat straw, when co-blended with PFR, exhibited a tendency to reduce the release of SO_2 compared to the OB sample blend. Similar findings were observed during the devolatilization phase.

Fig. 2c displays the correlation between the molar fuel-Si/Ca ratio and the release of H_2S or SO_2. To provide a baseline for comparison, non-blended components from [33] were also included in the plots. The results reveal a trend, where an increase in fuel-Si content is correlated with a higher release of both sulfur species. However, it is worth noting that the inhomogeneity of the biofuels led to the presence of outliers in the data, which, in turn, compromised the accuracy of the results.

On the other hand, an increased fuel-Ca content is associated with a reduction in the release of hydrogen sulfide or sulfur dioxide into the gas phase. These findings support the hypothesis regarding the interaction between the Si-network and the Ca cations, which influences the release of S-species during devolatilization and gasification.

Lastly, it is important to consider the impact of both Ca and K on the release of HCl. Fig. 2a illustrates the relationship between the molar Ca/K ratio and HCl release during devolatilization for the fuel blend materials analyzed. A distinct trend is observed: as the Ca/K ratio increases, the amount of HCl released during devolatilization decreases. These findings align with previous studies on industrially pre-treated wheat straw fuels [32]. In the high-temperature range (950 °C), Ca is primarily present as CaO, a major ash component, and it is possible that CaO acts as an HCl sorbent. Similar observations were reported by Shemwell et al. [43], who investigated the treatment of HCl gas with CaO, $CaCO_3$, and calcium formate, achieving removal efficiencies of

76%, 54%, and 81% respectively, depending on stoichiometry. A recent DFT study published in 2022 [44] explored the mechanism of HCl capture by CaO and suggested that the oxygen atoms on the surface of CaO play a crucial role in the adsorption of HCl.

It is plausible that a competitive mechanism exists between K and Ca. Thermodynamically, the formation of KCl is more favorable and stable than $CaCl_2$. Therefore, CaO can only bind additional HCl if there is no more K available in the gas phase. However, as discussed previously, there is an equilibrium with the silicates. This means that the explanation for this mechanism lies in the Ca/K ratio. However, depending on the amount of K relative to Cl, it may not work without Si or may be reduced to Ca+K.

3.3. Ash fusion behavior

All sample series were analyzed using hot stage microscopy (HSM) to investigate ash fusibility characteristics. Note that the fuel blends and their proportions were based on the feedstock itself. Fig. 3 illustrates the correlation between the coefficients h_x/h_0 of the sample ashes and temperature. Fig. 3a presents the ash melting curves for pre-treated barley straw without Ca-additive [33], while Fig. 3b depicts the materials with 2 wt% $CaCO_3$. It can be observed that the h_x/h_0 curves slightly decreased or increased within the low temperature range (600 °C to 700 °C). Apart from initial sintering effects, changes in volume may be attributed to residual carbon content in the ash interacting with CO_2 in the atmosphere. A comparison between the upgraded materials and the Ca-blended samples revealed significant effects on the h_x/h_0 curves. The ash from upgraded barley straw without Ca-additive displayed noticeable changes above 700 °C (excluding the untreated material itself). Conversely, the upgraded fuels blended with $CaCO_3$ demonstrated similar effects from approximately 1050 °C onwards. Thermal and leaching pre-treatments did not have a significant effect on ash behavior at 1050 °C, and the ash fusion behavior of the Ca-blended fuels remained unchanged. In other words, this suggests that only the presence of the Ca-additive had a decisive impact on the ash melting behavior by promoting the formation of high-melting calcium silicates, independent of the upgrading method. In addition, the Ca-additive appears to have a more significant impact on the ash fusion temperature compared to thermal and water-leaching treatment.

Fig. 3c illustrates the h_x/h_0 curves for raw colza straw samples blended with different proportions of PB. Interestingly, the sample blends showed similar ash fusion characteristics as observed for the raw colza straw ash, with ash melting occurring from a temperature range of 630 °C onwards. However, for the colza straw sample blended with 90 wt% PB, no effects were observed below 700 °C. Blends with a fraction of 75 wt% PB indicated noticeable effects below 650 °C, and samples with a fraction of either 25 wt% or 10 wt% PB were completely molten at 700 °C. It is not surprising that colza straw ash samples had relatively low melting points, considering that the source material itself had the highest fuel-K content and the lowest silicon fraction among all herbaceous biofuels investigated in [33]. In contrast, PB had a relatively low amount of fuel-K and a significantly higher silicon content compared to raw colza straw. Based on this fact, it can be reasonably assumed that dilution effects played a key role in the observed ash fusion characteristics. These findings indicate that simply blending K-rich feedstocks with woody components was not sufficient to positively affect the ash melting point. Comparing torrefied and postwashed colza straw blended with 35 wt% PB, it can be seen that the ash melting point was significantly increased. Since raw colza straw had a relatively low fraction of fuel-Si, high-melting silicates could not be formed regardless of whether the fuel-Ca content was significantly increased or not. Considering the

relatively high fuel-Ca content in raw colza straw, this further supports the evidence that high-melting calcium silicates cannot be formed without Si. Thus, this case highlights the difference between herbaceous feedstocks and emphasizes the need for individual upgrading approaches to influence ash chemistry accordingly. In such cases, the melting point could be successfully increased by adding biomass-based silicon-containing additives or blending components with a distinct silicon content.

Lastly, Fig. 3d displays the h_x/h_0 curves for torrefied and postwashed samples, which were further blended with woody feedstock components. A comparison with the upgraded fuel samples suggested that blending resulted in an increase in the ash melting point for the different sample varieties. For the upgraded fuels, ash melting was observed from temperatures above 700 °C, while the upgraded and co-blended samples exhibited an average melting temperature of 900 °C. The most promising results were obtained for corn straw blended with 30 wt% PB, while PFR showed the least effective results in terms of increasing the ash melting point. It should be noted that Corn/PB had the highest fuel-Si fraction among all samples examined (>1 wt%). This suggests that Si could form stable high-melting calcium silicates, which positively influenced the ash fusion temperature of the fuel samples. Additionally, biomass upgrading through postwashing had a significant side effect, as the fuel-K content was reduced by an average of half. Thus, the formation of low-melting potassium silicates was reduced, thereby diminishing the competition between Ca and K in terms of silicate formation.

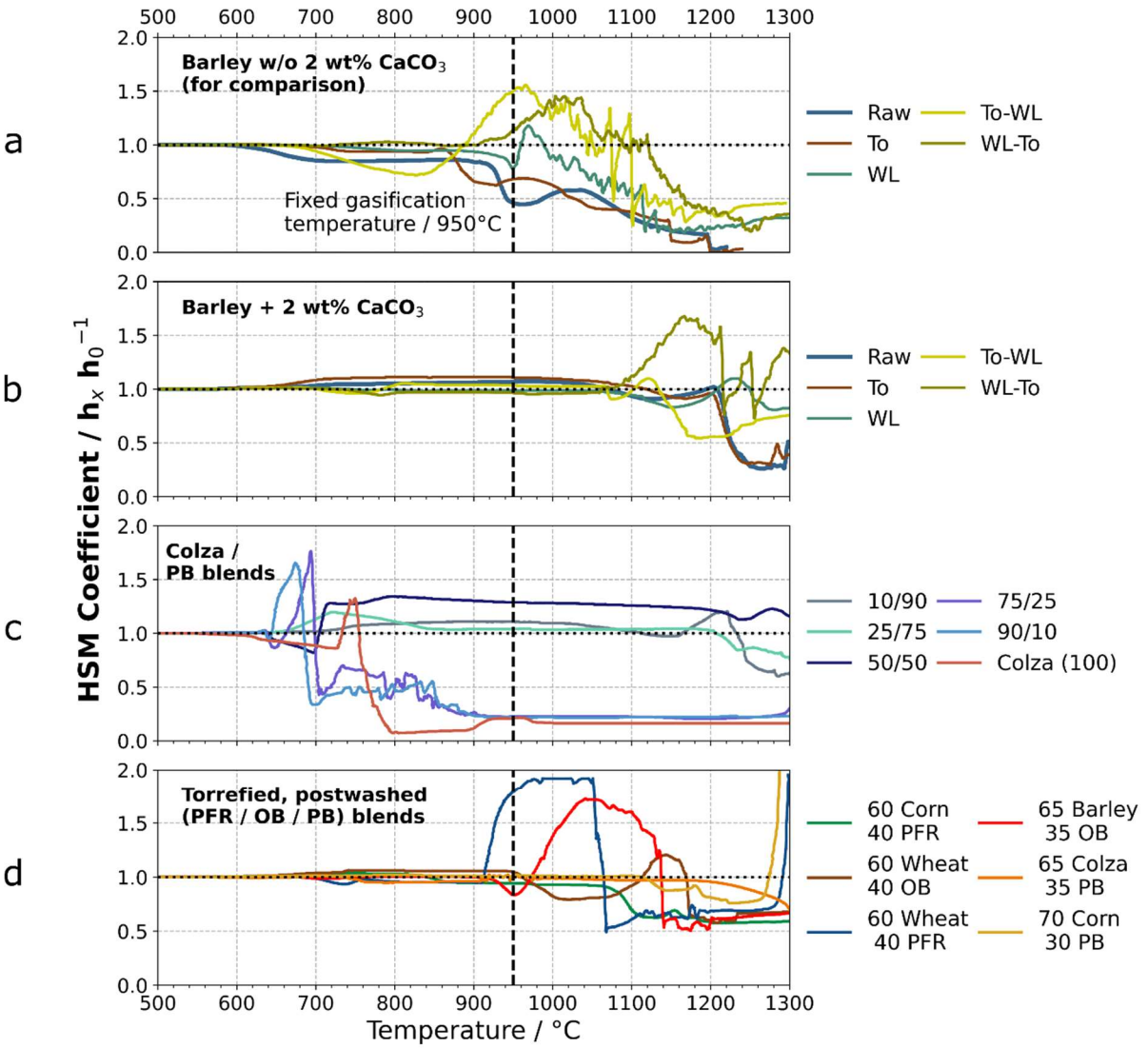

Fig. 3. Height profile (coefficient h_x/h_0) of ash samples determined by hot stage microscopy (HSM). **a** Upgraded barley straw without and with 2 wt% $CaCO_3$. **b** Untreated colza straw blended with varying proportions of PB. **c** Torrefied and postwashed straw varieties blended with woody components. Note that the non-blended components of biofuel (barley and colza straw), which have been included for comparison, were investigated in reference [33].

3.4. Thermodynamic modelling of the mineral phases' formation

The ash fusibility of the sample ashes is compared in ternary $CaO–K_2O–SiO_2$ diagrams in Fig. 4. Unlike solely upgraded barley straw (Fig. 4a), the Ca-blended samples showed distinct effects regarding their ash melting behavior. The green arrow indicates an increase in the fraction of CaO, and it is evident that the Ca-additive shifted the sample ash from the two-phase (solid and liquid) region to the solid phase, resulting in solid oxides being the dominant compounds. As a result, no ash melting should occur at the operating temperature of 950 °C. Previous experimental investigations conducted using HSM (Fig. 3b) have already confirmed the stability of the sample ashes at the specified gasification temperature.

Colza straw was mixed with different ratios of pine bark in its raw form, and a clear relationship between the blend proportions and the phase composition was observed (Fig. 4b). When colza straw had a proportion of 50 wt% to 75 wt% pine bark, the ash was found to be in the solid phase at the temperature of 950 °C, mainly due to the presence of the dominant oxide phase. Therefore, no ash melting should be expected. It appeared that this effect was primarily due to dilution effects, and the arrows in the diagram indicate a decrease in K_2O and a corresponding increase in SiO_2 with an increasing proportion of PB.

The last series of samples (Fig. 4c) focused on torrefied-postwashed straw varieties that were blended with woody components. It is worth noting that both woody components, OB and PFR, exhibited nearly identical phase compositions at 950 °C. In contrast to OB and PFR, PB was predicted to be in the two-phase region. Overall, it can be concluded that the most promising results in terms of increasing the proportion of solid oxides were achieved by blending upgraded barley straw with a Ca-additive, indicating that thermal stability can be expected at 950 °C. None of the Ca-blended samples investigated were found in the liquid phase. Furthermore, it appeared that simply blending the source material with Ca was sufficient to shift the ash constituents from the two-phase region to the solid phase, eliminating the need for any prior pretreatment to enhance this effect.

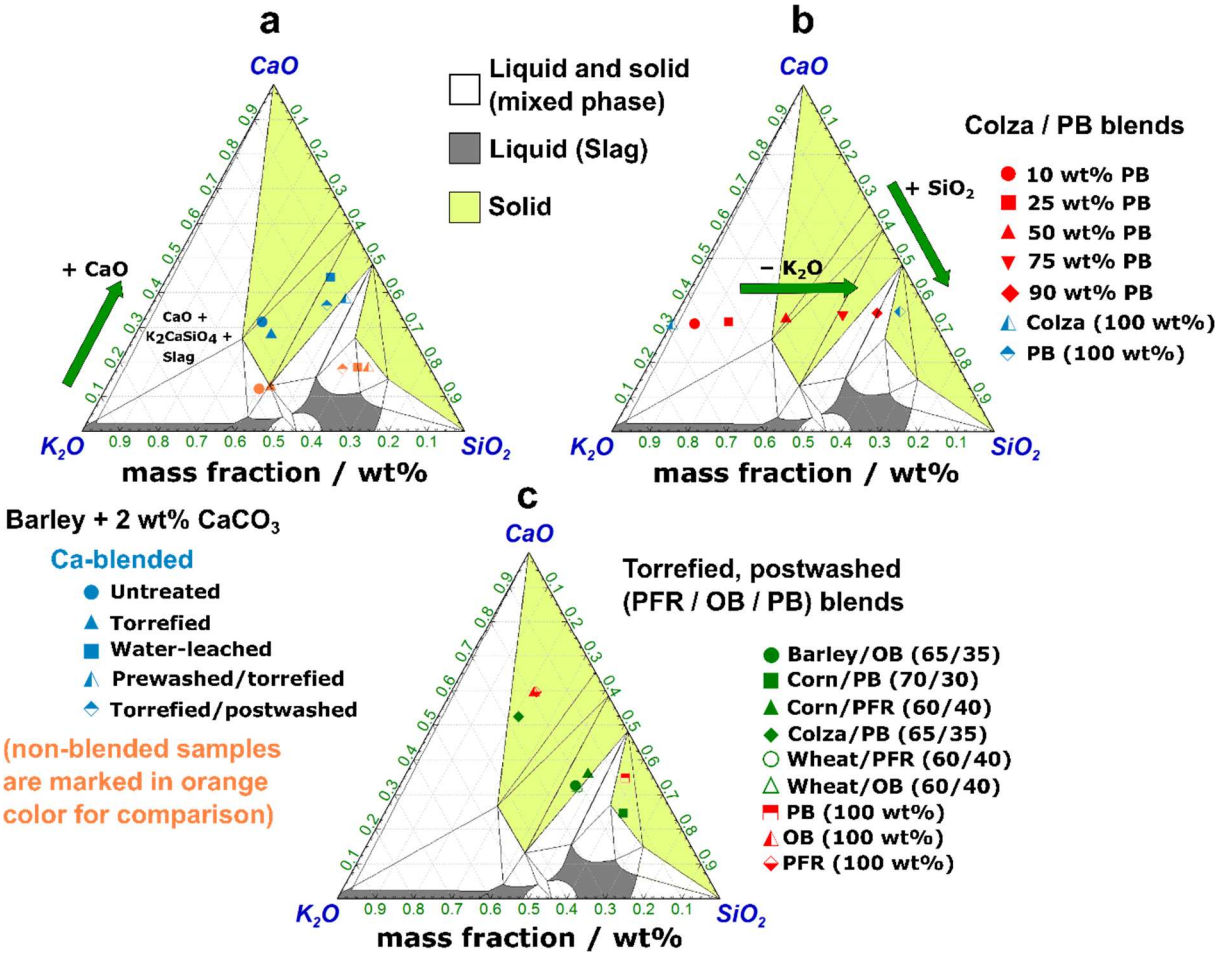

Fig. 4. Ternary phase diagrams for the SiO_2–CaO–K_2O system at 950 °C and atmospheric pressure, calculated using FactSage™ [45]. Predicted phase fields for ashes of pre-treated barley straw blended with 2 wt% $CaCO_3$ (**a**), colza straw blended with various proportions of PB (**b**), and torrefied-postwashed herbaceous straw varieties blended with various proportions of PB, OB, or PFR (**c**).

Mineral phase maps were predicted for all series of samples and are displayed in Fig. 5. The calculated phases for the torrefied-postwashed sample series are observed to align well with the experimental results (HSM, Fig. 3b). It is evident that the ashes from the colza/PB (65/35) and corn/PB (70/30) blends did not exhibit any signs of melting at 950 °C. HSM investigations confirmed the stability of both aforementioned sample blends within the specified temperature range, as no significant changes in sample specimen geometry were observed. However, the ash constituents of the residual sample blends were found to be situated close to the phase boundary between solid oxides and the two-phase region, albeit still in the solid phase. Consequently, they may exhibit thermal instability at 950 °C. On the other hand, these samples demonstrated a relatively high average melt fraction of approximately 75 wt%. Through experimental ash fusion testing using HSM, melting or expanding effects were indeed confirmed.

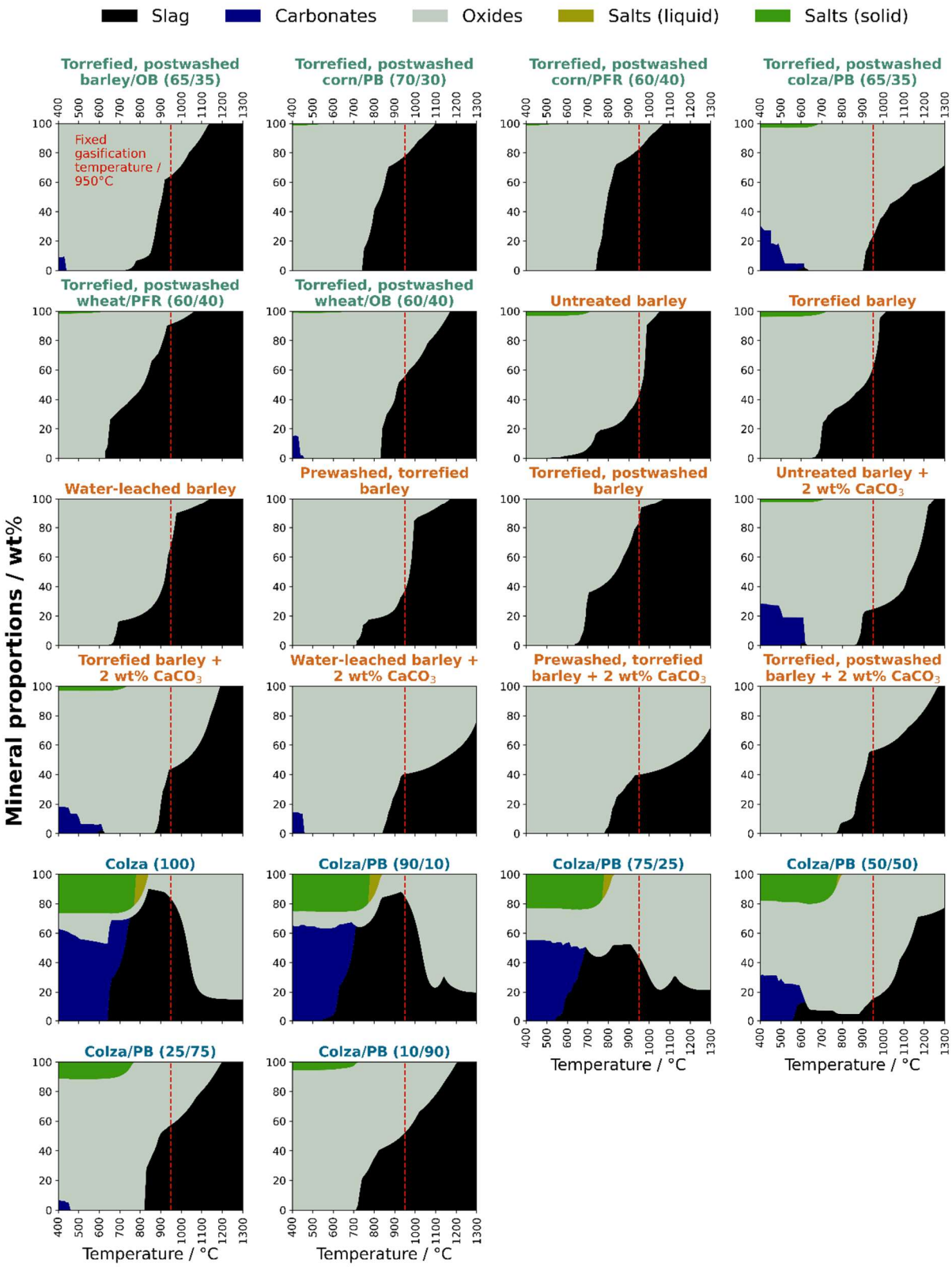

Fig. 5. Predicted mineral phase maps under gasification conditions for ashes of (upgraded) straw blends varieties. The dashed line represents the fixed gasification temperature of 950 °C.

In contrast to pre-processed barley straw, Ca-blended samples exhibited different phase formations at lower temperatures. Ca promoted carbonate formation, aligning well with the results obtained from the release experiments in Fig. 2a. A significant finding was the competition between K and Ca cations. It was hypothesized that Ca modified the silica network, thereby facilitating the formation of high-melting silicates. Consequently, the substitution of K by Ca resulted in an increased fraction of free K remaining in the ash. In their study, Novakovic et al. [46] reported on the release of K from the K-Ca-Si system. They discovered that at elevated temperatures, SiO_2 selectively reacted with CaO, leading to the release of more K into the gas phase rather than its incorporation into the silicate structure. In line with these findings, it can be suggested that K potentially formed carbonates instead, which could explain the absence of carbonates in the phase maps of pre- or post-washed samples. The carbonate fraction in the solely washed sample was considerably lower than that in the source material or the torrefied sample, indicating that most of the K was leached out during the washing treatment.

Regarding slag formation, Ca-blended barley straw samples have shown promising results. The formation of liquid slag was expected to begin between 800 °C and 850 °C and appeared to remain consistent up to 950 °C.

In the case of colza straw in its raw form and co-blended with increasing ratios of PB, there was a noticeable decrease in the formation of alkali salts (carbonates and chlorides) at lower temperatures with an increasing fraction of PB. This highlights the relatively high concentration of K in the ash of non-blended colza straw. The transition from solid carbonates to slag occurred smoothly, and based on the predicted thermodynamic activities of the species, the ash-slag mixture predominantly consisted of molten carbonates. It is important to note that both sample ashes, colza/PB (90/10) and colza/PB (75/25), exhibited a significant decrease in molten slag formation from around 950 °C onwards. This can be attributed to the increased release of components containing K, resulting in a reduction of slag. As a result, the majority of the formed slag can be attributed to high-temperature stable oxides, such as CaO. In this unique case, it should be mentioned that the investigated colza straw samples had a low silicon content (as seen in [33]), therefore no low-melting silicates were expected to form at high temperatures. On the other hand, an increased fraction of PB blend was accompanied by an increased concentration of silicon in the fuel. This led to a higher formation of molten slag when the PB fraction exceeded 25 wt%. Interestingly, even though there were lower amounts of fractional potassium and traces of sodium in the ash, which typically react with SiO_2 to produce low-melting substances, the ash still progressively fused from 950 °C onwards. Consequently, despite the higher proportion of the woody component (≥25 wt%) and the corresponding decrease in fuel-K, the potassium content in the fuel was still sufficient to form low-melting silicates at high temperatures.

In summary, the blending ratio of the woody component had significant effects on the phase formations in PB-blended colza straw samples, which were highly dependent on the ash forming constituents, especially K and Si. Ultimately, the findings clearly demonstrated the crucial role of chemical interactions between the inorganic components in determining the fusibility of the ash.

4. Conclusion and potential impacts on fluidized-be gasifier operation

The study thoroughly investigated the influence of a Ca-based additive and biofuel co-blending on the behavior of inorganic constituents. To predict the ash fusibility at 950 °C, ternary phase diagrams were created based on preliminary thermodynamic calculations. Sample series were then conceptualized. The Ca-based additive and the woody biofuel blending components were found to have significant effects on the formation of gas and mineral phases. The interactions of inorganics were attributed to both chemical effects and dilution.

It is evident that Si, Ca, and K play a crucial role in estimating slagging tendencies, making them fundamental factors for the slagging index. For instance, colza straw ash exhibits a relatively high fraction of KCl but a noticeable low level of fuel-Si. Compared to other herbaceous biofuels, the fraction of molten slag was found to be relatively low in the lower temperature range. Co-blending with woody biofuel components like PB had intriguing effects on ash fusion behavior, including the simultaneous reduction of molten slag formation and increase in the ash melting point. However, an excess of the PB blending component shifted the equilibrium chemistry to favor enhanced molten slag phases at lower gasification temperatures due to an excess of fuel-Si derived from the woody component. These findings emphasize the importance of comprehending the overall inorganic fuel composition.

In a recent study [32], notable correlations were observed between the Ca content in the fuel and the behavior of KCl release in batch-type experiments. This effect was further highlighted in our current work, as we directly compared Ca-blended barley straw with non-blended feedstock. These findings support the notion that Ca may contribute to the capture and deposition of gaseous alkali chlorides (KCl or NaCl) [47–49]. When the fuel sample was washed before blending with $CaCO_3$, there was a significant reduction in KCl release. Furthermore, Ca-blended barley straw exhibited a decrease in the release of sulfur species (such as H_2S, SO_2, and COS) into the gas phase compared to non-blended straw samples. The release of sulfuric species was also lower, as they were captured by available Ca. Therefore, the presence of Ca not only improved the ash melting behavior but also had potential technical benefits by chemically binding and preventing the release of KCl or S-containing species to the gas phase. Considering that H_2S has corrosive effects, the reduced release of H_2S can be a significant advantage for power plant operations due to its electrochemical nature.

Herbaceous feedstocks typically contain significant concentrations of Cl and S, which results in KCl and K_2SO_4 becoming the dominant K-containing compounds [41, 50]. Unlike silicates, especially KCl is relatively volatile. The release of this component can lead to increased deposition on heat transfer surfaces, which in turn reduces heat transfer and increases corrosion rates. Additionally, the release of these species into the gas phase can contribute to the formation of aerosols, such as "sub-micron" particles.

Furthermore, it was observed that fuels rich in calcium have an impact on the release behavior of HCl. In batch-type release experiments, there was a decrease in HCl release parallel to an increase in the fuel-Ca content. When the molar ratio of K was higher than Ca, more HCl was released since most K exists in the form of KCl in herbaceous feedstocks. Given that chlorine can accelerate high-temperature corrosion of reactor equipment during thermochemical conversion [51, 52], capturing HCl would have a favorable impact on this issue.

Colza/PB blends have demonstrated favorable effects on both their ash fusibility and the behavior of problematic species when the woody component PB comprises 50 wt% or more of the blend. This suggests that using woody-herbaceous fuel blends could be an interesting and cost-effective alternative to expensive chemical additives for controlling ash melting and the release behavior of inorganic compounds. Based on these findings, it is possible to produce valuable blends using low-cost fuels, which offers additional economic and ecological benefits by eliminating the need for additional chemical additives.

The removal of alkali species from high-temperature fuel gas is crucial for the smooth operation. Aluminosilicate minerals are commonly used as sorbent materials for alkali removal methods. On the other hand, Ca-based minerals like limestone are primarily used to increase the ash melting point by forming stable Ca-silicates with higher melting temperatures. Interestingly, the findings suggest that Ca-based additives also have unintentional positive effects in terms of S/Cl sorption mechanisms, which can have beneficial impacts on gas phase chemistry. Corrosion of reactor components and catalyst poisoning are mainly governed by volatile impurities such as chlorine and sulfur compounds in the gas phase. While the concentration of these impurities can be controlled to some extent through operational conditions and gasification processes, their presence remains an unavoidable issue during fluidized-bed operation. Chemical sorption therefore provides an additional advantage in reducing impurities and harmful pollutant emissions.

The addition of Ca-based additives and various biofuel blends has shown promising results in enhancing the thermal stability of ashes at 950 °C. The slag formation could be significantly reduced when blending barley straw with a Ca-additive. Additionally, whether or not thermal or water-leaching treatments were applied beforehand, the additive effectively increased the melting point of barley straw ash, as substantiated by both experimental analysis and thermodynamic modeling. As a result, this suggests that the issues related to slagging, fouling, and bed agglomeration in fluidized-bed gasifiers can be significantly mitigated.

In conclusion, it is important to acknowledge that the thresholds for classifying the quality of biofuels should be determined individually for each type of feedstock. This study clearly highlighted the differences in ash constituents and their concentrations among various herbaceous feedstocks. Therefore, additives or co-blending strategies should be specifically tailored to each feedstock. While predictive methods show promise in predicting ash fusion behavior and mineral phase formation at process temperatures, their application is maybe limited by kinetic constraints. Furthermore, it is worth noting that incorporating small amounts of cost-effective additives or blending with other biofuels is an attractive option for improving the quality of low-grade fuels. This approach allows for the utilization of a wider range of agricultural or biogenic residues. The use of additives and co-blending with woody fuel components has shown significant benefits in affecting both gas and mineral phases.

Author information

Corresponding Author

Florian Lebendig – Institute of Energy Materials and Devices (IMD-1), Forschungszentrum Jülich GmbH, Jülich 52428, Germany; orcid.org/0000-0003-4917-8275

Authors

Michael Müller – Institute of Energy Materials and Devices (IMD-1), Forschungszentrum Jülich GmbH, Jülich 52428, Germany

Notes

The authors declare no competing interests.

Acknowledgments

This research was funded by the Horizon 2020 Framework program of the European Union, CLARA project, G.A. 817841.

References

[1] Rogelj, J.; Popp, A.; Calvin, K. V.; Luderer, G.; Emmerling, J.; and Gernaat, D.; Fujimori, S.; and Strefler, J.; Hasegawa, T.; Marangoni, G.; et al. Scenarios towards limiting global mean temperature increase below 1.5°C. *Nature Climate Change* **2018**, *8*, 325–332.

[2] Friedlingstein, P.; Hauck, J.; Olsen, A.; Peters, W.; Pongratz, J.; Sitch, S.; Ciais, P.; Alin, S.; Aragão, L. E.; Arneth, A.; et al. Global carbon budget 2020. *Earth System Science Data* **2020**, *12*, 3269–3340.

[3] Sikarwar, V. S.; Zhao, M.; Clough, P.; Yao, J.; Zhong, X.; Memon, M. Z.; Shah, N.; Anthony, E. J.; Fennell, P. S. An overview of advances in biomass gasification. *Energy & Environmental Science* **2016**, *9*, 2939–2977.

[4] Condori, O.; De Diego, L. F.; Garcia-Labiano, F.; Izquierdo, M. T.; Abad, A.; Adánez, K. Syngas production in a 1.5 kWth biomass chemical looping gasification unit using Fe and Mn ores as the oxygen carrier. *Energy & Fuels* **2021**, *35*, 17182–17196.

[5] Mohamed, U. Zhao, Y.; Huang, Y.; Cui, Y.; Shi, L.; Li, C.; Pourkashanian, M.; Wei, G.; Yi, Q.; Nimmo, W. Sustainability evaluation of biomass direct gasification using chemical looping technology for power generation with and w/o CO_2 capture. *Energy* **2020**, *205*, 117904.

[6] Guo, Q.; Cheng, Y.; Liu, Y.; Jia, W.; Ryu, H.-J. Coal chemical looping gasification for syngas generation using an iron-based oxygen carrier. *Industrial & engineering chemistry research* **2014**, *53*, 78–86.

[7] Huseyin, S.; Wei, G.; Li, H.; Fang, H.; Huang, Z. Chemical-looping gasification of biomass in a 10 kWth interconnected fluidized bed reactor using Fe_2O_3/Al_2O_3 oxygen carrier. *Journal of Fuel Chemistry and Technology* **2014**, *42*, 922–931.

[8] Adanez, J.; Abad, A.; Garcia-Labiano, F.; Gayan, P.; De Diego, L. F. Progress in chemical-looping combustion and reforming technologies. *Progress in energy and combustion science* **2012**, *38*, 215–282.

[9] Nikolaisen, L. S.; Jensen, P. D. Biomass feedstocks: categorisation and preparation for combustion and gasification. *Biomass Combustion Science, Technology and Engineering* **2013**, Elsevier, 36–57.

[10] Keipi, T. Tolvanen, H.; Kokko, L.; Raiko, R. The effect of torrefaction on the chlorine content and heating value of eight woody biomass samples. *Biomass and Bioenergy* **2014**, *66*, 232–239.

[11] Meesters K.; Elbersen, W.; Van Der Hoogt, P.; Hristov, H. Biomass pre-treatment for bioenergy – Case study 5: Leaching as a biomass pre-treatment method for herbaceous biomass **2018**.

[12] Sami, M.; Annamalai, K.; Wooldridge, M. Co-firing of coal and biomass fuel blends. *Progress in energy and combustion science* **2001**, *27*, 171–214.

[13] Shi, J.; George, K. W.; Sun, N.; He, W.; Li, C.; Stavila, V.; Keasling, J. D.; Simmons, B. A.; Lee, T. S.; Singh, S. Impact of pretreatment technologies on saccharification and isopentenol fermentation of mixed lignocellulosic feedstocks. *BioEnergy Research* **2015**, *8*, 1004–1013.

[14] Boavida, D. Abelha, P.; Gulyurtlu, I.; Valentim, B.; De Sousa, M. J. L. A study on coal blending for reducing NO_x and N_2O levels during fluidized bed combustion. *International Journal of Energy for a Clean Environment* **2004**, *5, 175–191*.

[15] Williams, C. L.; Westover, T. L.; Emerson, R. M.; Tumuluru, J. S.; Li, C. Sources of biomass feedstock variability and the potential impact on biofuels production. *BioEnergy Research* **2016**, *9*, 1–14.

[16] Li, C.; Aston, J. E.; Lacey, J. A.; Thompson, V. S.; Thompson, D. N. Impact of feedstock quality and variation on biochemical and thermochemical conversion. *Renewable and Sustainable Energy Reviews* **2016**, *65*, 525–536.

[17] Boström, D.; Grimm, A.; Boman, C.; Björnbom, E.; Öhman, M. Influence of kaolin and calcite additives on ash transformations in small-scale combustion of oat. *Energy & Fuels* **2009**, *23*, 5184–5190.

[18] Hrbek, J.; Oberndorfer, C.; Zanzinger, P.; Pfeifer, C. Influence of $Ca(OH)_2$ on ash melting behaviour of woody biomass. *Carbon Resources Conversion* **2021**, *4*, 84–88.

[19] Werther, J.; Saenger, M.; Hartge, E.-U.; Ogada, T.; Siagi, Z. Combustion of agricultural residues. *Progress in energy and combustion science* **2000**, *26*, 1–27.

[20] Vuthaluru, H. B.; Zhang, D. K. Remediation of ash problems in fluidised-bed combustors. *Fuel* **2001**, *80*, 583–598.

[21] Llorente, M. J. F.; Cuadrado, R. E.; Laplaza, J. M. M.; García, J. E. C.. Combustion in bubbling fluidised bed with bed material of limestone to reduce the biomass ash agglomeration and sintering. *Fuel* **2006**, *85*, 2081–2092.

[22] Lindström, E.; Öhman, M.; Backman, R.; Boström, D. Influence of sand contamination on slag formation during combustion of wood derived fuels. *Energy & Fuels* **2008**, *22*, 2216–2220.

[23] Ray, A. E.; Li, C.; Thompson, V. S.; Daubaras, D. L.; Nagle, N.; Hartley, D. S. Biomass blending and densification: impacts on feedstock supply and biochemical conversion performance **2017**.

[24] Ou, L.; Luo, G.; Ray, A.; Li, C.; Hu, H.; Kelley, S.; Park, S. Understanding the impacts of biomass blending on the uncertainty of hydrolyzed sugar yield from a stochastic perspective. *ACS Sustainable Chemistry & Engineering* **2018**, *6*, 10851–10860.

[25] Jacobson, J. J.; Roni, M. S.; Lamers, P.; Cafferty, K. G. Biomass feedstock and conversion supply system design and analysis. *INL* **2014**.

[26] Dutta, A.; Sahir, A. H.; Tan, E.; Humbird, D.; Snowden-Swan, L. J.; Meyer, P. A.; Ross, J.; Sexton, D.; Yap, R.; Lukas, J. Process design and economics for the conversion of lignocellulosic biomass to hydrocarbon fuels: Thermochemical research pathways with in situ and ex situ upgrading of fast pyrolysis vapors. *PNNL* **2015**.

[27] Jones, S.; Meyer, P.; Snowden-Swan, L.; Padmaperuma, A.; Tan, E.; Dutta, A.; Jacobson, J.; Cafferty, K. Process design and economics for the conversion of lignocellulosic biomass to hydrocarbon fuels: fast pyrolysis and hydrotreating bio-oil pathway. *NREL* **2013**.

[28] Awoyale, A. A.; Lokhat, D. Experimental determination of the effects of pretreatment on selected Nigerian lignocellulosic biomass in bioethanol production. *Scientific reports* **2021,** *11*, 1–16.

[29] Tu, R.; Jiang, E.; Yan, S.; Xu, X.; Rao, S. The pelletization and combustion properties of torrefied Camellia shell via dry and hydrothermal torrefaction: a comparative evaluation. *Bioresource technology* **2018**, *264*, 78–89.

[30] Yu, C.; Thy, P.; Wang, L.; Anderson, S. N.; VanderGheynst, J. S.; Upadhyaya, S. K.; Jenkins, B. M. Influence of leaching pretreatment on fuel properties of biomass. *Fuel Processing Technology* **2014**, *128*, 43–53.

[31] Zheng, A.; Zhao, Z.; Chang, S.; Huang, Z.; Zhao, K.; Wei, G.; He, F.; Li, H. Comparison of the effect of wet and dry torrefaction on chemical structure and pyrolysis behavior of corncobs. *Bioresource technology* **2015**, *176*, 15–22.

[32] Lebendig, F.; Funcia, I.; Pérez-Vega, R.; Müller, M. Investigations on the Effect of Pre-Treatment of Wheat Straw on Ash-Related Issues in Chemical Looping Gasification (CLG) in Comparison with Woody Biomass. *Energies* **2022**, *15*, 3422.

[33] Lebendig, F.; Müller, M. Effect of pre-treatment of herbaceous feedstocks on behavior of inorganic constituents under chemical looping gasification (CLG) conditions. *Green Chemistry* **2022**, *24*, 9643–9658.

[34] Lebendig, F.; Schmid, D.; Karlström, O.; Yrjas, P.; Müller, M. Influence of pre-treatment of straw biomass and additives on the release of nitrogen species during combustion and gasification. *Renewable and Sustainable Energy Reviews* **2024**, *189*, 114033.

[35] Bläsing, M.; Müller, M. Mass spectrometric investigations on the release of inorganic species during gasification and combustion of German hard coals. *Combustion and flame* **2010**, *157*, 1374–1381.

[36] Bläsing, M.; Zini. M.; Müller, M. Influence of feedstock on the release of potassium, sodium, chlorine, sulfur, and phosphorus species during gasification of wood and biomass shells. *Energy & fuels* **2013**, *27*, 1439–1445.

[37] Pang, C. H.; Hewakandamby, B.; Wu, T.; Lester, E. An automated ash fusion test for characterisation of the behaviour of ashes from biomass and coal at elevated temperatures. *Fuel* **2013**, *103*, 454–466.

[38] Bale, C. W.; Bélisle, E.; Chartrand, P.; Decterov, S. A.; Eriksson, G.; Gheribi, A. E.; Hack, K.; Jung, I.-H.; Kang, Y.-B.; Melançon, J.; et al. Reprint of: FactSage thermochemical software and databases, 2010–2016. *Calphad* ***2016***, *55*, 1–19.

[39] Yazhenskikh, E.; Jantzen, T.; Hack, K.; Müller, M. A new multipurpose thermodynamic database for oxide systems. *Rasplavy/Melts* **2019**, *2*, 116–124.

[40] Müller, M.; Wolf, K.-J.; Smeda, A.; Hilpert, K. Release of K, Cl, and S species during co-combustion of coal and straw. *Energy & fuels* **2006**, *20*, 1444–1449.

[41] Niu, Y.; Tan, H.; et al. Ash-related issues during biomass combustion: Alkali-induced slagging, silicate melt-induced slagging (ash fusion), agglomeration, corrosion, ash utilization, and related countermeasures. *Progress in Energy and Combustion Science* **2016**, *52*, 1–61.

[42] Wu, H.; Pedersen, M. N.; Jespersen, J. B.; Aho, M.; Roppo, J.; Frandsen, F. J.; Glarborg, P. Modeling the use of sulfate additives for potassium chloride destruction in biomass combustion. *Energy & fuels* **2014**, *28*, 199–207.

[43] Shemwell, B.; Levendis, Y. A.; Simons, G. A. Laboratory study on the high-temperature capture of HCl gas by dry-injection of calcium-based sorbents. *Chemosphere* **2001**, *42*, 785–796.

[44] Ma, X.; Huang, X.; Feng, T.; Mu, M.; Hu, X. A DFT study on the mechanism of HCl and CO_2 capture by CaO. *Reaction Chemistry & Engineering* **2022**, *7*, 758–768.

[45] Bale, C. W.; Chartrand, P.; Degterov, S. A.; Eriksson, G.; Hack, K.; Mahfoud, R. B.; Melançon, J.; Pelton, A. D.; Petersen, S. FactSage thermochemical software and databases. *Calphad* **2002**, *26*, 189–228.

[46] Novaković, A.; van Lith, S. C.; Frandsen, F. J.; Jensen, P. A.; Holgersen, L. B. Release of potassium from the systems K-Ca-Si and K-Ca-P. *Energy & Fuels* **2009**, *23*, 3423–3428.

[47] Wang, L.; Skjevrak, G.; Hustad, J. E.; Skreiberg, Ø. Investigation of biomass ash sintering characteristics and the effect of additives. *Energy & Fuels* **2014**, *28*, 208–218.

[48] Åmand, L.-E.; Leckner, B.; Eskilsson, D.; Tullin, C. Deposits on heat transfer tubes during co-combustion of biofuels and sewage sludge. *Fuel* **2006**, *85*, 1313–1322.

[49] Pettersson, A.; Zevenhoven, M.; Steenari, B.-M.; Åmand, L.-E. Application of chemical fractionation methods for characterisation of biofuels, waste derived fuels and CFB co-combustion fly ashes. *Fuel* **2008**, *87*, 3183–3193.

[50] Glarborg P.; Marshall, P. Mechanism and modeling of the formation of gaseous alkali sulfates. *Combustion and Flame* **2005**, *141*, 22–39.

[51] Kassman, H.; Broström, M.; Berg, M.; Åmand, L.-E. Measures to reduce chlorine in deposits: Application in a large-scale circulating fluidised bed boiler firing biomass. *Fuel* **2011**, *90*, 1325–1334.

[52] Saidur, R.; Abdelaziz, E. A.; Demirbas, A.; Hossain, M. S.; Mekhilef, S. A review on biomass as a fuel for boilers. *Renewable and sustainable energy reviews* **2011**, *15*, 2262–2289.

Table of Contents (TOC) Graphic